A Model for Solar Coronal Mass Ejections

S. K. Antiochos

E.O. Hulburt Center for Space Research, Naval Research Laboratory, Washington, DC, 20375

C. R. DeVore

Laboratory for Computational Physics and Fluid Dynamics, Naval Research Laboratory, Washington, DC, 20375

and

J. A. Klimchuk

E.O. Hulburt Center for Space Research, Naval Research Laboratory, Washington, DC, 20375

Received _____; accepted _____

ABSTRACT

We propose a new model for the initiation of a solar coronal mass ejection (CME). The model agrees with two properties of CMEs and eruptive flares that have proved to be very difficult to explain with previous models. a) Very low-lying magnetic field lines, down to the photospheric neutral line, can open toward infinity during an eruption. b) The eruption is driven solely by magnetic free energy stored in a closed, sheared arcade; consequently, the magnetic energy of the closed state is well above that of the post-eruption open state. The key new feature of our model is that CMEs occur in multi-polar topologies, in which reconnection between a sheared arcade and neighboring flux systems triggers the eruption. In this "magnetic breakout" model, reconnection removes the unsheared field above the low-lying, sheared core flux near the neutral line, thereby allowing this core flux to burst open. We present numerical simulations which demonstrate that our model can account for the energy requirements for CMEs. We discuss the implication of the model for CME/flare prediction.

Subject headings:

1. Introduction

It is now widely recognized that coronal mass ejections (CMEs) are the most important manifestation of solar activity that drives the space weather near Earth (Gosling 1993, Gosling 1994). CMEs are huge ejected plasmoids, often with masses $\gtrsim 10^{16}$ g and energies $\gtrsim 10^{32}$ ergs, and frequently subtending more than 60° in position angle (*e.g.* Howard *et al.* 1985, Hundhausen 1997). Recently, certain LASCO coronagraph observations from SOHO have been interpreted as evidence that CMEs can be global disruptions completely circling the Sun (Brueckner 1996, Howard *et al.* 1997). In addition to being the primary cause of major geomagnetic disturbances, CMEs are also a fundamental mechanism by which the large-scale corona sheds flux and, hence, may play a central role in the solar cycle. Therefore, an understanding of the mechanism for CME initiation has long been a primary goal of solar physics theory.

There are a number of basic observational constraints that any theoretical model for CME initiation must satisfy. Since the plasma beta in the non-flaring corona is typically small, $\beta \sim 10^{-2}$, gas pressure alone cannot be the driver. Early models for CMEs proposed that the eruption is driven by explosive flare heating, but it is now known that many CMEs occur with little detectable heating, especially those originating from high-latitude quiet regions. It has also been proposed that CMEs may be due to magnetic buoyancy effects (*e.g.,* Low 1994, Wu, Gou, & Wang 1995, Wolfson & Dlamini 1997), but this would imply CMEs should be associated with large masses of falling material. During prominence eruptions, material can sometimes be observed to fall back onto the chromosphere, but CMEs often occur with negligible prominence activation and very little evidence for downward moving plasma. Coronagraph observations usually show all the CME plasma moving outward, in which case buoyancy is unlikely to be the driver. These considerations have led most investigators to conclude that the energy for the eruption must be stored in

the magnetic field.

The general topology of a CME appears to be that of an erupting arcade overlying a photospheric neutral line (*e.g.* Martin & McAllister 1997). The magnetic field near CME neutral lines is observed to run almost parallel to the line, indicating that the field is far from potential. This magnetic stress is commonly referred to as "shear", and is most likely the source of energy for the eruption. Note that the actual type of arcade can range from low-lying kilogauss fields associated with filament eruptions and flares in active regions to weak high-latitude fields associated with polar crown filaments.

Since many CMEs are accompanied by the ejection of prominences or filaments, it appears that the innermost flux of the erupting arcade opens out to the solar wind. The question of whether all the arcade flux opens or whether some inner field is left closed is a critical one for theoretical models (Aly 1991, Sturrock 1991, Wolfson & Low 1992, Mikić & Linker 1994). All the field that is observed above the occulting disk of present coronagraphs, ($\geq 1.1R_{\odot}$), is observed to open, but there may remain a considerable amount of closed arcade flux below this height. Since low-lying active region filaments sitting on the chromospheric neutral line are observed to be ejected, we believe that for some eruptions all the arcade flux down to the chromospheric neutral line must open. Others have argued, however, that the field reconnects back down to a closed state just as the filament begins to lift, so that the innermost flux near the chromosphere never actually opens. This issue remains to be resolved observationally.

As will be discussed in detail below, requiring all the arcade flux to open imposes an extreme constraint on theories for CMEs. It is much easier to explain the eruption if a significant fraction of the flux remains closed. The key feature of the model presented in this paper is that it can produce an eruption in which even the innermost arcade flux at the photospheric neutral line can open to infinity and, yet, the eruption is purely magnetically

driven.

Another observational constraint on theoretical models is that the stressing of the coronal magnetic field is slow compared to characteristic time scales in the corona. Photospheric driving velocities are typically of order 1 km/s, whereas characteristic coronal speeds are of order several hundred km/s for sound waves and several thousand km/s for Alfvenic motions. Therefore, to a good approximation, the energy for a CME is pumped into the corona quasi-statically.

This quasi-static evolution of the corona is controlled by two processes: the displacement of magnetic footpoints by photospheric and sub-photospheric flows, and the emergence and submergence of magnetic flux through the photosphere. It is not clear which process is most important for producing the shear, or whether both play significant roles depending on the type of solar region. Many CMEs originate in coronal helmet streamers, which often swell for several days before the eruption (Hundhausen 1997). Such swelling often is attributed to shearing of the magnetic footpoints (*e.g.* Klimchuk 1990), although the emergence of new flux also could produce this effect. For the model proposed in this paper, it is irrelevant whether the shear is due to photospheric flows or to flux emergence. The key requirement is that the stressing is slow. In the simulations presented below, boundary flows were used to generate the shear, but we expect the same results if shear emergence is used. The major advantage to our boundary conditions is that they are straightforward to understand and completely physical. As emphasized by a number of authors (*e.g.* Aly 1984, Klimchuk & Sturrock 1989, Wolfson & Verma 1991), a low-β system like the corona is highly sensitive to boundary conditions at the base, and the application of inappropriate conditions can easily lead to erroneous conclusions about the equilibrium of the coronal field. By driving the shear with slow footpoint motions we are assured that any eruption that occurs is physically valid and not an artifact of peculiar boundary conditions. Note

that the boundary conditions we use are exactly the ones used by Aly, Sturrock, and others in deriving the energy limit.

The final constraint on CME theories is that the corona has no upper boundary. Field lines are allowed to expand to infinity if it is energetically favorable for them to do so. This seems like a trivially obvious statement, but it has profound implications for the possible evolution of the magnetic field.

Taken together, the constraints of an open corona and of quasi-static stressing make it very difficult to understand how violent eruptions can occur on the Sun. Intuitively, one would expect the field to respond to slow photospheric driving by simply expanding outward to infinity rather than by undergoing a violent eruption. This intuition is confirmed by a number of numerical simulations which have shown that sheared 2.5D force-free bipolar arcades in Cartesian geometry do not erupt as long as physically appropriate boundary conditions are assumed (Klimchuk & Sturrock 1989, Finn & Chen 1990, Wolfson & Verma 1991). There is also no evidence for eruption in 2.5D bipolar arcades in spherical geometry (Roumeliotis, Sturrock, & Antiochos 1994). The sheared field simply expands outward, pushing any overlying flux outward as well, and approaches the open state asymptotically with increasing shear (Sturrock, Roumeliotis, & Antiochos 1995). Eruptions can be obtained if significant resistivity is present (Biskamp & Welter 1989, Steinolfson 1991, Inhester, Birn, & Hesse 1992, Mikić & Linker 1994), but contrary to observations, the field opens only partially and disconnected plasmoids form in the corona.

The basic problem encountered by all the numerical models to date is that, irrespective of the magnitude of the shear, the closed configurations that the models compute contain less magnetic energy than the fully open state. In fact, Aly and Sturrock have claimed, on the basis of mathematical arguments, that the maximum energy state of any force-free field is the fully open field (Aly 1984, Aly 1991, Sturrock 1991). Although this claim has

not been proved completely rigorously, it is in agreement with every numerical simulation (including the ones in this paper) and, hence, seems very likely to be correct. In order to obtain a CME, however, we need more energy in the pre-eruption sheared state than in the final open state, since energy is needed not only to open the field, but also to accelerate and lift the plasma against gravity. The energy going into the plasma can be very large, of order 10^{32} ergs or more; hence, the energy in the pre-eruption field must be well above the energy of the fully open state – a result which appears to be in direct conflict with the Aly-Sturrock limit.

2. The Theoretical Model

We propose in this paper a CME model that can resolve the apparent contradiction between the Aly-Sturrock energy limit and CME observations. Let us first clarify why Aly-Sturrock, in fact, requires that previous models be in conflict with observations. Since a number of observations indicate that CMEs can occur over extremely long neutral lines, sometimes apparently circling the whole Sun (Brueckner 1996), and since most CME and/or flare associated activity appears to occur along a single neutral line on the photosphere, models for CMEs and eruptive flares generally assume a 2.5D bipolar magnetic geometry with either translational or azimuthal symmetry. Hence, the magnetic system consists of a single coronal arcade (*e.g.* Roumeliotis, Sturrock, & Antiochos 1994, Mikić & Linker 1994).

The important point is that, for a single arcade system, the observational requirement that the innermost flux near the neutral line open up requires that *all* the flux in the system open. But this is forbidden by the Aly-Sturrock limit, at least, for a purely magnetically-driven eruption, because no sheared field state can have enough energy to open up all the flux. The only way to obtain an eruption in these models is by the formation of closed plasmoids in the corona, so that some of the flux is disconnected

from the photosphere. The Aly-Sturrock arguments do not apply to topologies with disconnected flux. But in the real 3D corona, reconnection will not result in the formation of disconnected flux from the photosphere. In 3D the Aly-Sturrock energy limit will apply and is likely to suppress any eruption of a single arcade even in the presence of reconnection, as in the so-called tether-cutting model (*e.g.* Sturrock 1989, Moore & Roumeliotis 1992). Furthermore, it is very difficult to see how 3D reconnection in a single arcade can lead to the opening of the innermost flux near the neutral line. We conclude that any single arcade model is doomed to failure.

Let us consider, instead, a multi-flux system such as the field shown Figure 1a. In this case we have three neutral lines on the photosphere and four distinct flux systems: a central arcade straddling the equator (blue field lines), two arcades associated with the neutral lines at $\pm 45°$ (green field lines), and a polar flux system overlying the three arcades (red lines). Note that there are two separatrix surfaces which define the boundaries between the various flux systems, and a null point on the equatorial plane at the intersection of the separatrices.

Suppose that, as a result of large shear concentrated at the equatorial neutral line, a CME occurs and the innermost flux of the central arcade opens up. The difference now is that, even if the system is strictly 2.5D, the innermost flux can open down to the neutral line at the equator without opening all the flux in the system and without the formation of disconnected flux. Clearly, there is no reason for a shear that occurs only near the equator to affect the high-latitude (green) arcades; therefore, their flux should remain closed throughout the evolution. But this is not significant energetically, since the green arcades are not expected to play an important role in constraining the eruption. The key point is that much of the flux of the central (blue) and overlying (red) systems also can remain closed during eruption. If reconnection between red and blue field lines occurs at the null

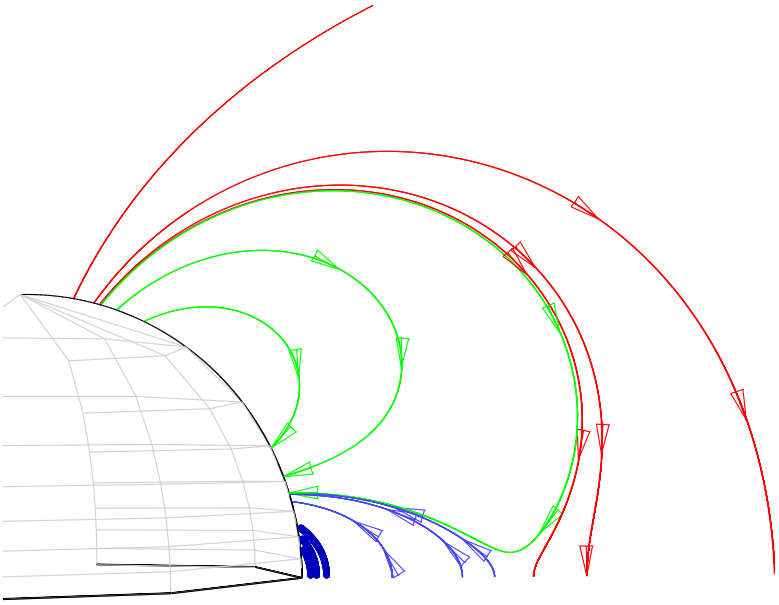

Fig. 1(a) Initial potential magnetic field. The field is symmetric about the axis of rotation and the equator, so only one quadrant is shown. The photospheric boundary surface is indicated by the light grey grid. Magnetic field lines are colored (red, green, or blue) according to their flux system. Two types of blue field lines are indicated, higher-lying light-blue unsheared field and low-lying dark-blue field which is sheared later in the simulation.

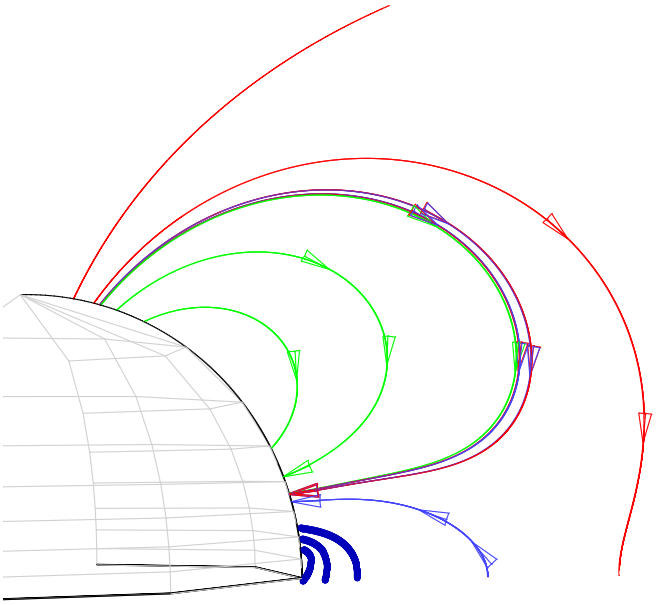

Fig. 1(b) The force-free field after a shear of $\pi/8$. The field lines shown correspond to those in 1a. They are traced from the same footpoint position on the photosphere as in 1a.

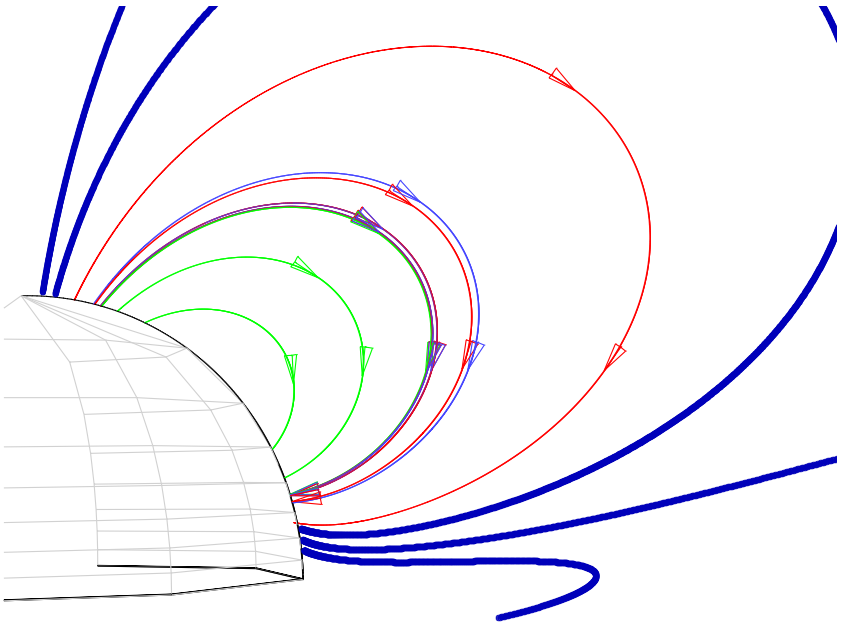

Fig. 1(c) As above, but for a shear of $3\pi/8$.

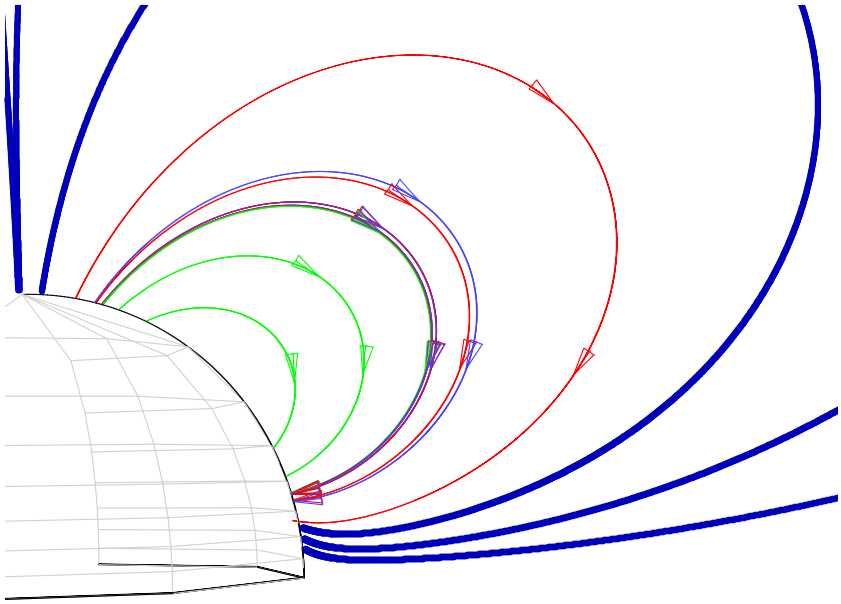

Fig. 1(d) As above, but for a shear of $\pi/2$.

point, this reconnection will result in the transfer of flux from the blue and red systems to the side (green) arcades. Such a flux transfer allows unsheared blue and red flux to get out of the way of the erupting sheared core flux, but still remain closed. Note that this process is possible only in a multi-flux system. In a single arcade system all the unsheared flux is forced to open because it basically has nowhere else to go.

Flux transfer in a multi-polar system also allows us to understand how a large energy excess sufficient to power a CME can be built up in a closed sheared field and, yet, be compatible with the Aly-Sturrock limit. The key point is that the "fully" open state is not unique in a multi-polar system. To illustrate, let E_{max} denote the energy of that state in which all the flux initially in the central and overlying arcades (blue and red) opens, but the green flux remain closed. When the shear is confined only to the arcade at the equator, E_{max} is the appropriate energy limit rather than the larger energy corresponding to all the flux, including green, being open. Note that the state with energy E_{max} can be reached by a purely ideal evolution in which the sheared core field expands slowly outward pushing all the overlying flux out to infinity, with no reconnection at the null. The side flux is distorted by the expanding field, but does not open. The final state has a current sheet at the equator reaching down to the photosphere, and a current sheet at the top of each side arcade, so that each green side arcade becomes a helmet streamer.

We expect that no sheared closed configuration can have energy above E_{max}, so if it were the only state accessible, there would be no eruption, just as in the single arcade case. If we allow reconnection at the null, however, then other open states with lower energy become accessible. For example, if the shear is confined to a small latitudinal band $\pm\Theta$ near the equator and well inside the separatrix of the blue arcade, then consider the state in which the flux inside $\pm\Theta$ opens, while as much as possible of the rest of the flux in the system is closed. (It may not be possible for all the unsheared blue flux to be closed,

because there may not be sufficient red flux for the blue to reconnect with.) Let this state, which has the minimal amount of open flux, have energy E_{min}. The open state E_{min} looks very similar to the state E_{max}, except that the distribution of flux between the open and closed systems is different. We can consider E_{max} and E_{min} to be the maximally and minimally open states respectively. The important point is that the magnitude of E_{min} can be much less than E_{max}, because the state E_{min} may contain much less open field.

We propose that the energy for CMEs and eruptive flares is due to this difference between E_{max} and E_{min}. If the reconnection at the null is slow, then the energy in the sheared closed configuration can rise well above E_{min}. It can never go above E_{max}, but depending on the ratio of sheared flux to unsheared flux in the central arcade, the energy of the sheared closed field could be much larger than E_{min} so there could be a large amount of energy available for eruption.

In this model the unsheared blue and red fluxes act to confine the expansion of the sheared core field. We expect that a CME (or eruptive flare) occurs when reconnection at the null weakens this confinement sufficiently, so that the sheared field starts to expand outward rapidly, driving ever faster reconnection at the null and "breaking out" to infinity. Note that this magnetic "breakout" model naturally implies explosive-type behavior.

A crucial issue for our model is the rate of reconnection at the null. If this rate is fast, faster than the rate at which the system is being sheared (either by photospheric flows or flux emergence), then the magnetic energy always stays below E_{min} and no eruption can occur. We expect, however, that the reconnection will be slow at first because the shear occurs only far from the separatices. Under these circumstances a quasi-static evolution should be possible, so that only weak currents develop near the null and separatrices. If so, there should be negligible reconnection, and the energy in the system may rise well above E_{min}. In the next section we present numerical simulations which confirm this hypothesis.

3. Numerical Simulations

3.1. Force-Free Field Calculations

In order to test the free energy issue discussed above, we calculated the energy of a sheared multipolar field using two procedures. First, we calculated the energy E_{min} by determining the minimum-energy force-free field for a given distribution of shear at the photosphere. The use of a force-free calculation needs some clarification. Since the field has a null point, the true evolution cannot be force-free because any finite gas pressure will dominate near the null. Hence, the force-free simulations do not determine a physical evolution for the system. We use the force-free code only as a convenient method for calculating the equilibrium state corresponding to the minimum magnetic energy for a given shear on the field and in the limit of vanishing gas pressure.

The important feature of the force-free calculations is that they include the effects of reconnection. The numerical algorithm that the code uses to solve the force-free equations is basically iterative relaxation (Yang, Sturrock, & Antiochos 1986). Given the positions of all the field line footpoints on the boundary, and some initial guess at the solution in the interior, the code iterates the solution monotonically towards the minumum energy state. However, the code uses a multi-grid procedure, so that the relaxation is first performed on very coarse grids with poor resolution and, consequently, high numerical diffusion. This means that the iteration process allows for reconnection, in that flux will transfer rapidly from one flux system to the other as long as this transfer is consistent with the boundary conditions and results in a decrease in the magnetic energy. Note that there is no real diffusion in the system, however, because there is no slippage of the footpoints at the solar surface. The shear is strictly enforced by the boundary conditions, but the field is free to reconnect at will across the null in order to reach its absolute minimum energy state.

The code solves the force free equations,

$$(\nabla \times \vec{B}) \times \vec{B} = 0, \tag{1}$$

using an Euler potential representation for the field (Yang, Sturrock, & Antiochos 1986). Azimuthal symmety is assumed, so that

$$\vec{B} = \nabla\alpha(r,\theta) \times \nabla\left(\phi - \gamma(r,\theta)\right). \tag{2}$$

The advantage of the Euler representation is that the photospheric shear is specified directly by the value of γ at the photosphere, $r = 1$. By fixing γ there, we fix the shear irrespective of how the field changes in the interior.

For the initial, unstressed (potential) field (Figure 1a), we assumed a multipolar flux distribution given by,

$$\alpha(r,\theta) = \frac{\sin^2\theta}{r} + \frac{(3 + 5\cos 2\theta)\sin^2\theta}{2r^3}. \tag{3}$$

The field consists of a dipolar component which dominates at large r, and an octopolar component at the surface. In the middle corona, $r \sim 2$, the field appears quadrupolar with an X-type null point on the equatorial plane. Due to the 2.5D symmetry of our system, the normal flux at the photosphere is unchanged by the shear and, hence, the value of α at the lower boundary is constant: $\alpha(1,\theta) = (5/4)\sin^2 2\theta$. Note that the flux maximum $\alpha = 1.25$ occurs at the neutral line at $\theta = \pi/4$.

From Eqtns (2) and (3) we find that,

$$B_r(r,\theta) = \frac{1}{r^2\sin\theta}\frac{\partial\alpha}{\partial\theta}. \tag{4}$$

so that the normal field at the photosphere is given by $B_r(1,\theta) = 10\cos\theta\cos 2\theta$, which implies that there are three neutral lines located at $\theta = \pi/4$, $\pi/2$, and $3\pi/4$. The position of the null point on the equatorial plane can be determined from the requirement that B_θ vanish there. From (2) and (3) we find that $B_\theta(r,\pi/2) = r^{-3} - 3r^{-5}$, consequently the null is

located at $r = \sqrt{3}$. The value of the flux function at the null, $\alpha(\sqrt{3}, \pi/2) = 2/(3\sqrt{3}) = .385$, from which we find that the separatrices intersect the northern hemisphere at $\theta = .2941$ and 1.277. Note that we have chosen the form of α so that positive flux in each hemisphere exactly balances the negative flux there, while α vanishes at the poles and equator. This means that there is exactly enough red flux to reconnect with all the blue flux, if such reconnection were energetically favored.

The imposed shear is assumed to be antisymmetric about the equator, and confined to a small latitudinal band there; *i.e.*,

$$\gamma(1, \theta) = \begin{cases} \chi\, C(\psi^2 - \Theta^2)^2 \sin\psi, & \text{for } \psi < \Theta \\ 0 & \text{for } \psi \geq \Theta, \end{cases} \tag{5}$$

where $\psi = (\pi/2 - \theta)$ is the solar latitude, $\Theta = \pi/15$ is the assumed latitudinal extent of the shear layer, and $C = 8.68252 \times 10^3$ is a normalization constant chosen so that $\gamma = \chi$ at the latitude of maximum shear, $\psi = .094$. The form of $\gamma(1, \theta)/\chi$ is shown in Figure 2. Note that the boundary of the shear layer occurs at $\theta = 13\pi/30$, where $\alpha = .207$, whereas the value of α at the boundary of the blue arcade (the separatrix) is .385. Hence, only about half the flux of the central arcade is sheared.

We solved the force-free equations above in the domain ($1 \leq r \leq 100$, $0 \leq \theta \leq \pi/2$) using a 512×512 non-uniform grid. Due to the symmetry of the system about the equatorial plane, only one hemisphere needed to be calculated. The grid was selected to enhance the resolution near the solar surface and near the equator, in particular, the grid points were spaced uniformly in x and y, where $x = \ln r$ and $y = \exp(6\,\theta/\pi)$. The boundary conditions at the pole $\theta = 0$ and the equator $\theta = \pi/2$ were set by symmetry. At the inner boundary $r = 1$, the shear profile $\gamma(1, \theta)$ was specified using the form above, and the flux distribution $\alpha(1, \theta)$ was fixed to its initial value. At the outer boundary $r = 100$ both $\alpha(100, \theta)$ and $\gamma(100, \theta)$ were fixed to their initial value. This meant that there was no shear at the outer

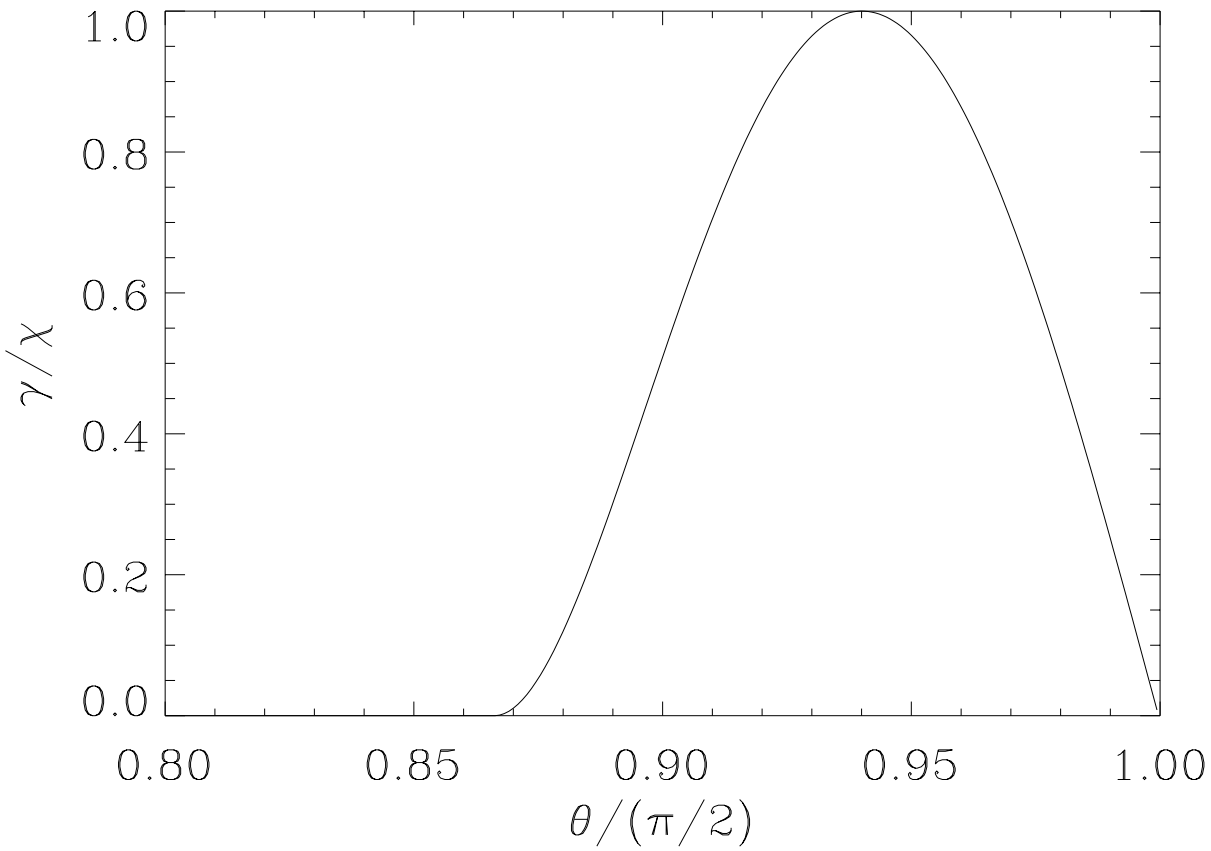

Fig. 2. The normalized shear profile as a function of colatitude.

boundary, $\gamma(100, \theta) = 0.$, which is a good assumption, because the sheared field lines were initially very far from the outer boundary. However, fixing α at the outer boundary means that no flux is allowed to exit the system. This is not valid since as the inner core field expands, it will push on the outer field lines so that even the flux very far from the solar surface will move outward. The amount of flux at $r = 100$ is very small, however, and the energy associated with this flux is so small that the outer boundary conditions have a negligible effect on the structure and energetics of the system, even for shears much larger than the values we discuss below.

The results of the force-free field calculation for three shear values, $\chi = \pi/8$, $\pi/4$, and $\pi/2$, are shown in Figures 1b, c, and d. The field lines in all these figures were traced beginning at exactly the same footpoint positions as in Figure 1a, in which there are 4 footpoints in the red system, 3 green footpoints, 3 light-blue (unsheared), and 3 dark-blue (sheared). The color of the field lines in Figures 1b - 1d corresponds to the initial color of the footpoints, irrespective of whether reconnection has occurred. Even for a low shear of $\pi/8$, it is evident that some reconnection has taken place since two of the red and two of the light-blue field lines have now joined the green system. It should be noted that, although the maximum shear is $\pi/8$, the average over the shear layer is only about half this value. For $\chi = \pi/2$ almost all the blue flux has reconnected with the red and has expanded outward far from its initial position. Therefore, we expect the energy of the $\pi/2$ sheared state to be close to that of the open state, E_{min}. In fact, we have continued the force-free calculations to shears twice this value and find almost no increase in the magnetic energy. It can be seen in Figure 3 that the energy of the force-free field appears to saturate at a maximum value of approximately 6% above the initial potential field energy, *i.e.* $E_{min} = 1.06 E_{pot}$. Note that the 6% figure refers to the total energy of the initial field, including all the unsheared arcades. If we consider only the energy initially in the central, blue arcade, the relative energy increase is over an order of magnitude larger.

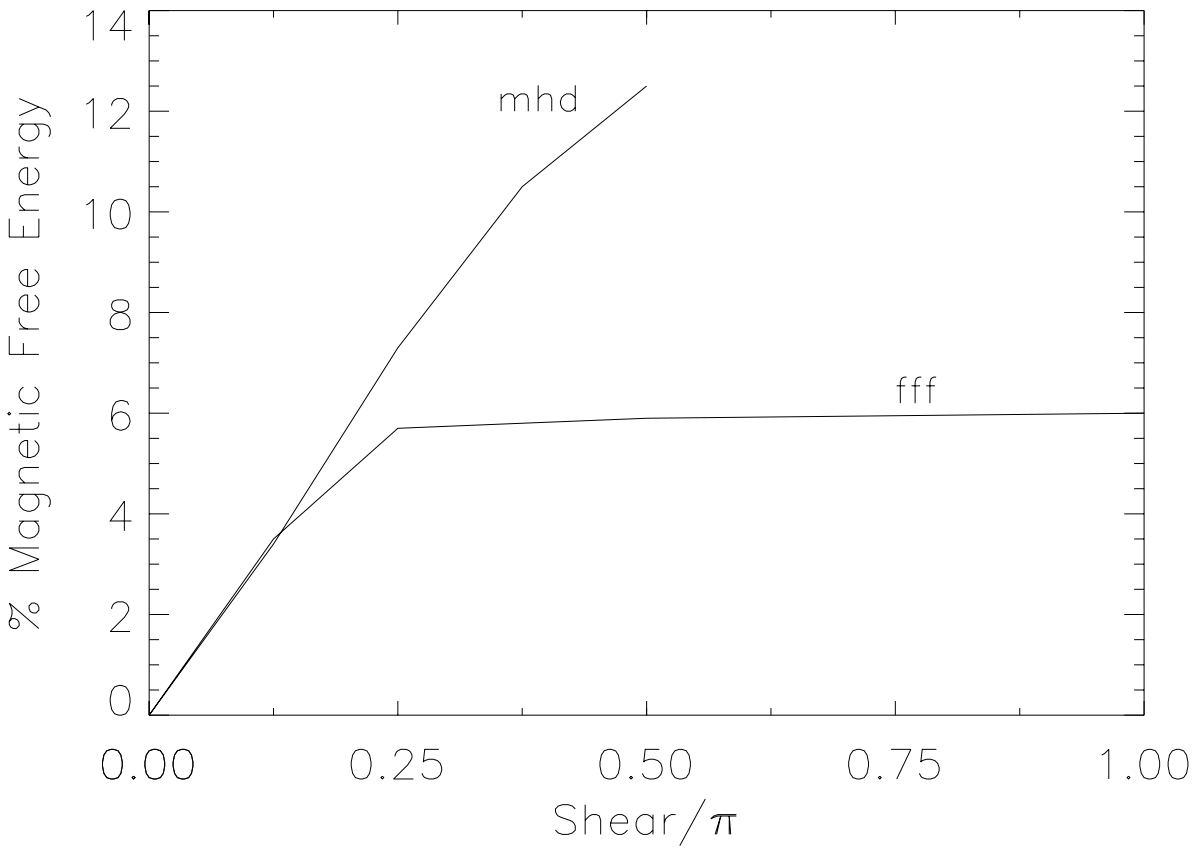

Fig. 3. The magnetic free energy as a function of shear for the force-free field solution (lower curve) and the MHD solution (upper curve). The shear is in units of π and the free energy is expressed as percentage of the initial, potential field energy.

An issue that requires clarification is how the force-free calculations determine a sequence of equilibrium states leading to the state E_{min}. The code finds the absolute minimum energy state for a given shear at the base, assuming that reconnection occurs freely at the null. For small shear only the unsheared light-blue field lines reconnect, as in Fig. 1b, but as the shear increases the outermost sheared field line eventually reaches the null. It is important to emphasize that the sheared field lines (dark-blue) also reconnect freely. This is evident from Figs. 1c and 1d. The dark-blue lines have reconnected and now have one of their footpoints near the pole. Although these lines have reconnected, they have not lost their shear. The footpoint displacement γ is strictly maintained at the photosphere by the boundary conditions. This is also physically valid. As long as the system has small resistivity, the reconnection will occur in a region of negligible volume (a current sheet), and the field reconnects with negligible diffusion. In this case the reconnected field lines maintain their footpoint displacement (Karpen, Antiochos, & DeVore 1996). Note also that all field lines with a footpoint in the shear zone, even if the field line has joined the green system, continue to expand outward toward the open configuration as the shear increases. In the limit of infinite shear, the field achieves the open state E_{min} in which all the field lines in the shear zone (by now they have all become part of the green systems due to reconnection) and any left over red field lines open.

3.2. MHD Calculations

The results of our force-free calculations determined the magnitude of E_{min}. The key question is whether a sheared coronal field will evolve to a state with energy significantly above this value, or whether reconnection at the null keeps the energy below E_{min}. In order to calculate the physical evolution for the field, we performed a fully time-dependent simulation using a 2.5D ideal MHD code in spherical coordinates developed by DeVore

(1991). The code uses a multi-dimensional FCT algorithm for transporting the conserved quantities, and maintains the divergence free condition on the magnetic field to machine accuracy.

The code solves the standard ideal MHD equations appropriate for the solar corona:

$$\frac{\partial \rho}{\partial t} + \nabla \cdot (\rho \vec{v}) = 0 \tag{6}$$

$$\frac{\partial}{\partial t}(\rho \vec{v}) + \nabla \cdot (\rho \vec{v}\vec{v}) + \nabla P = \frac{1}{4\pi}(\nabla \times \vec{B}) \times \vec{B} - \rho g_{\odot} R_{\odot}^2 \frac{\vec{r}}{r^3} \tag{7}$$

$$\frac{\partial U}{\partial t} + \nabla \cdot (U \vec{v}) + P \nabla \cdot \vec{v} = 0 \tag{8}$$

$$\frac{\partial \vec{B}}{\partial t} = \nabla \times (\vec{v} \times \vec{B}) \tag{9}$$

where ρ is mass density, $\vec{v}$ is velocity, P is gas pressure, $\vec{B}$ is magnetic induction, $g_{\odot}$ is the solar surface gravity (2.75×10^4 cm/s^2), $R_{\odot}$ is the solar radius (7.0×10^{10}cm), and U is the internal energy ($U = 3P/2$).

We use exactly the same initial magnetic field and shear profile as in the force-free calculations, but now we must also specify the initial plasma distribution. The plasma was taken to be in hydrostatic equilibrium, with initial temperature and density given by

$$T(r) = \frac{2 \times 10^6}{r^7} \text{ K}, \quad \text{and} \quad \text{n(r)} = \frac{2 \times 10^8}{\text{r}} \text{ cm}^{-3}. \tag{10}$$

Since the field drops off rapidly with radius, these forms for T and n were chosen in order to keep the plasma $\beta \equiv 8\pi P/B^2$ from becoming too large at large distances from the surface. Although the values of β in our simulation are not as low as those in the real corona, they are definitely less than unity near the bottom boundary. The values for T and n above imply an initial plasma pressure at the solar surface of 5.5×10^{-2} ergs/cm^3. The field strength at the surface ranges from a value of $B = B_r = 10$ at the pole, so that $\beta = .014$ there, to $B = B_\theta = -2$ at the equator where $\beta = .35$. Once we begin shearing, the value

of β drops much lower. Of course the system is always high-beta near the null point, so it deviates substantially from the force-free case there.

We use the same non-uniform grid as in the force-free calculations, except that the outer boundary is placed at $r = 10$ rather than at $r = 100$. As will be shown below, the field does not expand outward as much in the MHD case, so there is less influence from the outer boundary. Furthermore, we assume open boundary conditions there, so that flux and mass are free to move past the outer boundary. The use of a smaller domain allows us to have higher spatial resolution, which turns out to be the limiting factor in the MHD simulations. The boundary conditions at the polar axis and the equatorial plane are determined, as before, by symmetry considerations. At the inner boundary, the photosphere, we assume a line-tied impenetrable surface with an imposed azimuthal velocity given by the shear profile above and with a sinusoidal temporal profile.

A critical parameter is the magnetic Reynolds number R_M. Our fully-2D FCT transport algorithm uses higher order differencing so that, as in all finite-difference codes, the effective Reynolds number is quite high: $R_M >> 10,000$, as long as the magnetic and plasma structure is well resolved numerically. Of course, these values for R_M are still small compared to classical solar values. If structure develops on the scale of the grid spacing, then the effective R_M drops to become of order the number of grid points ~ 500. We conclude, therefore, that our simulation only overestimates (greatly) the true rate of reconnection that would occur on the Sun.

We drove the system with a sequence of shear motions applied at the photospheric boundary. Each shear phase had a sinusoidal time profile with a period of 25,000 s and a maximum footpoint displacement of $\pi/8$. For this period and amplitude the maximum shear velocity at the photosphere is approximately 10 km/s, whereas the Alfven speed is approximately 500 km/s in the model corona. Hence, the evolution was nearly quasi-static

until the very end of the simulation when large velocities appeared near the null due to reconnection.

The resulting field lines at the end of the first shear phase are shown in Figure 4a. These field lines are traced from exactly the same footpoint positions as the lines in Figure 1a. We note that the field lines in Fig. 4a have pushed outward as a result of the shear, but unlike the corresponding force-free case (Fig. 1b) there is no evidence for reconnection yet in the MHD results. The MHD system does appear to have achieved a true equilibrium. We let the system relax for an additional 50,000 s, and the resulting field was virtually indistinguishable from that in Fig. 4a. We conclude that there are at least two magnetostatic equilibria that the system can achieve for a given shear. One is the force-free state of Fig. 1b, in which the field outside the sheared region is current-free and the null is a true X-point with right-angle separatrix lines. This state has the lowest energy, but it can be reached only with reconnection. Another solution is the MHD state of Fig. 4a, in which no reconnection occurs at the null. In this case the unsheared field cannot be current-free, so that gas pressure, and perhaps gravity, must play a role in the force balance. We can infer from Fig. 4a that the separatrix surfaces are not quite perpendicular to each other, which indicates there is some weak current near the null. This current, however, is less than 1% of the maximum current in the shear region.

Figures 4b, c, and d show the results of the MHD simulation after three more shear phases. The solution in Fig. 4c corresponds to a total maximum shear in each hemisphere of $3\pi/8$. Although no noticeable reconnection has ocurred, the field at the null becomes progressively distorted from a right-angle X-type neutral point. The reason for this is straightforward. To relieve their stress, blue field lines expand outward towards an open configuration, pushing the overlying red lines outward as well. The green field lines, on the other hand, are unstressed and have no interest in being dragged out to infinity, so they

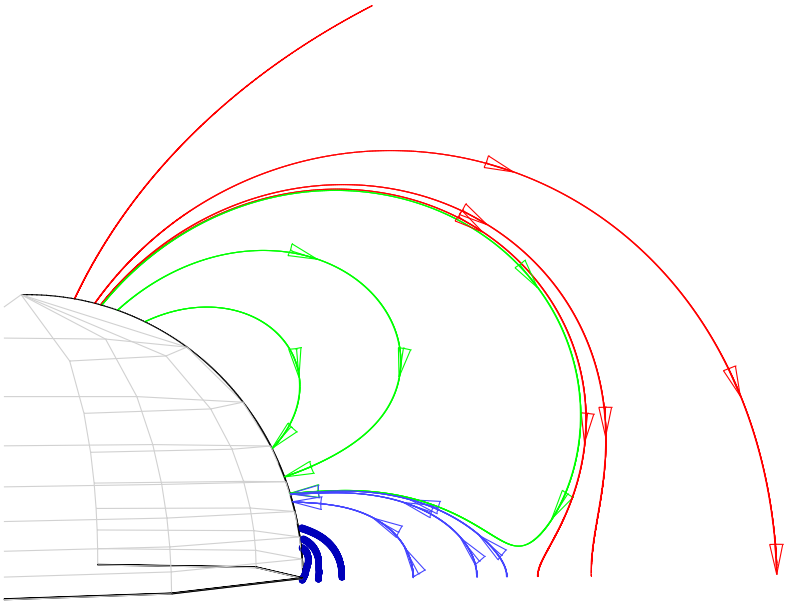

Fig. 4(a) The MHD solution after a shear of $\pi/8$. The field lines shown are the same as those in Figure 1.

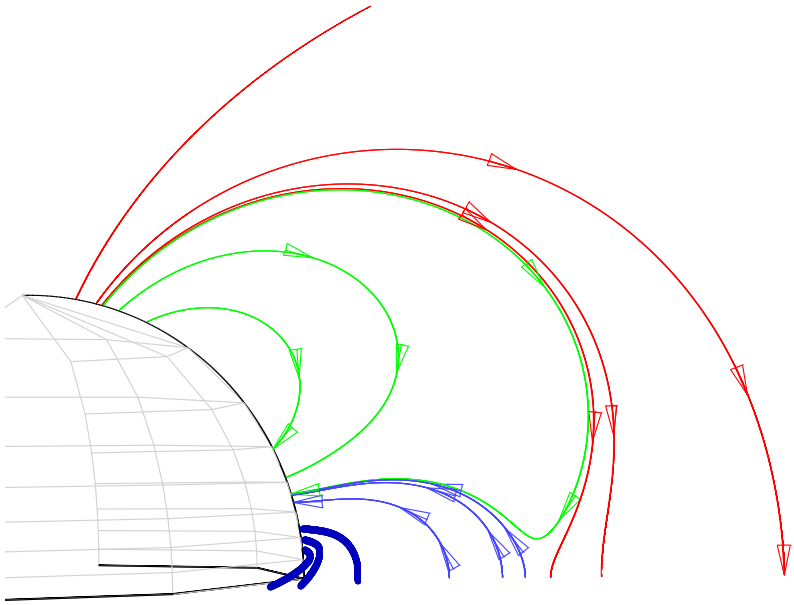

Fig. 4(b) As above, but for a shear of $\pi/4$.

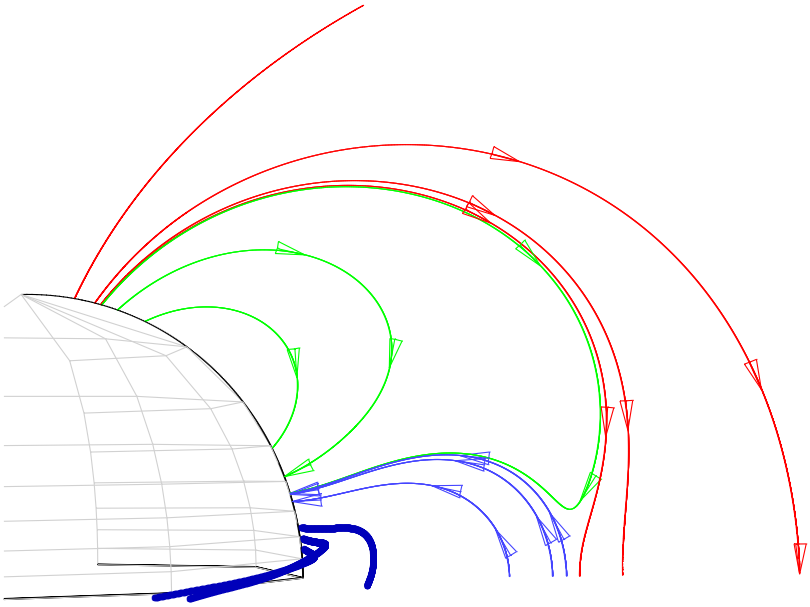

Fig. 4(c) As above, but for a shear of $3\pi/8$.

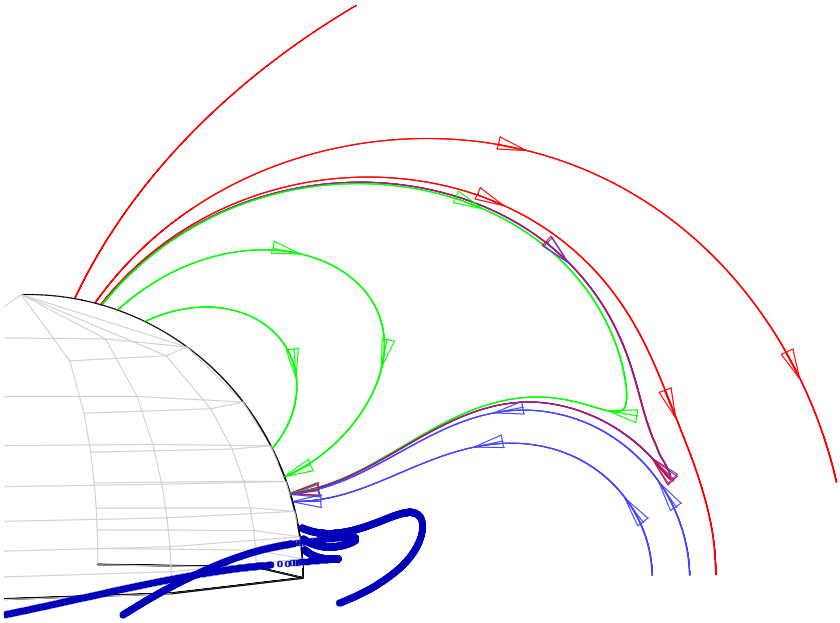

Fig. 4(d) As above, but for a shear of $\pi/2$.

simply move aside by pulling away from the neutral point. Consequently, the separatrix lines become more and more oblique, as blue and red flux push towards each other while green pulls away.

We can gain some insight into the evolution of the structure near the null point by considering a simple analytic model. Curvature effects can be neglected sufficiently near the null and a locally Cartesian coordinate system can be used. Let the origin of this coordinate system be at the null, the x axis be horizontal (parallel to the equatorial plane), and the y axis be vertical. If the field near the null has no shear, then an appropriate form for the potential α (see Equation (2)) there is:

$$\alpha(x, y) = B_0 \left(\frac{y^2}{2l_y} - \frac{x^2}{2l_x} \right), \tag{11}$$

where l_x and l_y are two constants that determine the scale of the gradients in x and y respectively. The separatrix lines are given by $\alpha = 0$; consequently, if $l_x = l_y$, these lines are perpendicular to each other, and as we show below, the current vanishes. From this form for α we derive a magnetic field,

$$\vec{B} = B_0 \left(\frac{y}{l_y}\hat{x} + \frac{x}{l_x}\hat{y} \right), \tag{12}$$

and an electric current density,

$$\vec{J} = B_0 \frac{l_y - l_x}{l_x l_y} \hat{z}. \tag{13}$$

Note that if $l_x = l_y$ then the current vanishes and we recover the right-angle X-type null point of a potential field. If the scales are not equal, then there is a finite current in the system which implies a finite Lorentz force given by,

$$\vec{J} \times \vec{B} = B_0^2 \frac{l_y - l_x}{l_x l_y} \left(-\frac{x}{l_x}\,\hat{x} + \frac{y}{l_y}\,\hat{y} \right). \tag{14}$$

Assuming that gravity is negligible, then the Lorentz force must be balanced by the pressure gradient, which implies that the pressure is given by,

$$P = P_0 + \frac{B_0^2}{4\pi} \frac{l_y - l_x}{l_x l_y} \left(-\frac{x^2}{2l_x} + \frac{y^2}{2l_y} \right), \tag{15}$$

where P_0 is the gas pressure at the null.

Initially the field is current-free and $l_x = l_y$, but as the field is distorted by the outward expanding blue flux, the angle formed by the separatrix surfaces becomes more and more acute so that l_x becomes smaller than l_y. In the limit that $l_x << l_y$, Equations (12) -(14) above imply that, $\vec{B} \rightarrow (B_0 x/l_x)\hat{y}$, $\vec{J} \rightarrow (B_0/l_x)\hat{z}$, and $P \rightarrow P_0 - (B_0^2/8\pi)(x^2/l_x^2)$. In other words, the null deforms to a classical current sheet. This trend is clearly evident in Fig. 4.

From our investigations of single dipole fields (Roumeliotis, Sturrock, & Antiochos 1994, Sturrock, Roumeliotis, & Antiochos 1995) we expect that at large shear, the red and blue field lines expand outwardly exponentially with increasing shear and, consequently, the current sheet thins out exponentially fast. This implies that reconnection eventually must begin to occur here, and once this reconnection starts it should accelerate. Our simulation shows convincing evidence for this type of evolution. There is no sign of reconnection at a shear of $3\pi/8$ (Fig. 4c). We let the field relax for an additional 30,000 s after this shearing phase, and saw no change in the field structure; hence, the field in Fig. 4c is also a true equilibrium. At a shear of $\pi/2$, however, the current structure at the null becomes only a few grid cells wide and reconnection begins. For example, in Fig. 4d some of the red and blue lines clearly have reconnected and joined the green flux system. The simulation could find no equilibrium for this shear. When we tried to let the system relax by continuing the simulation beyond the shearing phase, the reconnection became progressively stronger with magnetic islands appearing at the interface between the red and blue systems. The velocities there became very large and the density plummetted, halting the simulation.

Although our code could not simulate the actual eruption, it did prove the key result that the energy of the sheared MHD field greatly exceeds E_{min}. In Figure 3 we compare the magnetic energies as a function of shear for the force-free and MHD solutions. One may question the validity of such a comparison because the MHD simulation also includes

the effects of the plasma energy, however, the change in plasma thermal energy during the whole shearing phase (before appreciable reconnection) was less than 10% of the magnetic energy change. It is evident from Fig. 3 that the MHD solution energy exceeds E_{min} even for a shear of $\pi/4$, while the free energy of the MHD solution is approximately twice that of E_{min} for a shear of $3\pi/8$. Therefore, there is no way for the system to evolve to its minimum energy state except by transferring this excess energy to the plasma, *i.e.* by a violent eruption.

4. Discussion

The most important result of the MHD simulation is that contrary to many other calculations, current sheets do not form at the separatrix until late in the shearing. There are two reasons for this result. First, no shear is applied at the separatrix. This is the main difference between this simulation and other simulations, including our own (*e.g.,* Karpen, Antiochos, & DeVore 1996, Karpen, Antiochos, & DeVore 1998). If a shear were to be applied at the separatrix of our configuration, then a discontinuous B_ϕ would be created due to the discontinuity in relative footpoint positions, and a current sheet would immediately appear, just as in the previous simulations. But we apply a shear only near the neutral line, far from the separatrix. In fact, the field outside the shear region should always be nearly current-free for our 2.5D system since a quasi-static force-free approximation should be valid everywhere except near the null, and an unsheared 2.5D force-free field must be potential. This is exactly what our simulation finds, the current is completely negligible except in the shear region and in the high-β region around the null.

Second, discontinuities do not appear at the null, itself, because we include in our model a finite plasma pressure so that the system is far from force-free near the null. In order to calculate the evolution of the null in the first place, the plasma pressure and

dynamics must be fully included. Without the plasma the null could not even change its position. The null moves outward only because stress is transmitted from the field to the plasma in the low-β region, imparting momentum to the plasma, which then moves the field in the high-β region around the null. The plasma pressure is also essential for a smooth equilibrium to form. As the inner flux system expands outward it compresses the plasma in the high-β region around the null, increasing the plasma pressure there until force balance is achieved, as in the simple analytic model described above. It is only when the null region is squeezed down to the dissipation length scale, which corresponds to a few grid points in our numerical system, that significant reconnection begins and equilibrium becomes impossible to maintain. Of course, on the Sun the magnetic Reynolds number is very large, and the dissipation scale is many orders of magnitude smaller than global scale of the magnetic field.

An interesting implication of this discussion is that the exact energy equation for the plasma must play a crucial role in determining when eruption will occur. In the simulation we assumed a simple adiabatic energy equation (8), but radiation losses, thermal conduction, and ohmic heating may all be important. If the plasma at the null cools as it compresses, then the width of the null region can decrease rapidly to the dissipation scale. On the other hand, if the plasma heats then the null region resists compression and reconnection will be delayed. Hence, we have the very interesting situation that the dynamics of huge phenomena such as CMEs may be controlled by detailed plasma processes occurring in relatively tiny regions.

Another interesting property of our "magnetic breakout" model for CME initiation/flare triggering is that it involves several observable features which could form the basis for an effective prediction scheme. One feature is that the shear is concentrated near the neutral line, in agreement with observations (Schmieder *et al.* 1996) and with our theory

for prominence formation (Antiochos et al. 1994). Note that the shear responsible for eruptions cannot be due to differential rotation since that would preferentially shear long, high-lying flux rather than the short, low-lying flux near the neutral line. Differential rotation would produce the opposite shear profile from that shown in Figure 2. The upcoming Solar-B mission should be able to measure the magnetic shear at the photosphere with great accuracy, and determine the relation, if any, between shear distribution and eruptive activity.

Another feature of the model is that multiple flux systems must be present in order for an eruption to occur. It is well known that large eruptive flares only occur in complex topologies, in particular δ-spot regions. It can be shown that a δ-spot has a 3D magnetic topology of a four-flux system, exactly analogous to the 2.5D model discussed here (Antiochos 1998). We propose that this explains why δ-spots are so flare productive, whereas bipolar spot regions are not. Note that this provides a clear distinction between our breakout model and the usual tether-cutting model (*e.g.* Sturrock 1989, Moore & Roumeliotis 1992). Since the tether-cutting model involves only a single arcade, it would predict that a strongly sheared bipolar spot region is just as likely to flare as a δ-spot region.

CMEs also favor magnetic complexity. Both Mauna Loa and LASCO observations indicate that CMEs are more common in regions where the coronal field has a multipolar structure, rather than a simple bipolar structure (McAllister, Hundhausen, & Burkepile 1995, Schwenn *et al.* 1996). In addition, observations suggest that many CMEs involve more than one neutral line and, therefore, more than one flux region (Webb et al. 1997).

On the other hand, there are numerous examples of high-latitude CMEs that appear to involve only a bipolar magnetic topology. It would seem that this type of event contradicts the breakout model. However, the high-latitude CMEs not associated with active regions are invariably slow, with height-time profiles similar to that of the slow solar wind rather

than flare-associated ejection (*e.g.* Sheeley *et al.* 1997). We propose that this type of CME should not be considered a coronal mass **ejection**, but merely a coronal mass **expansion**. The key point is that, if the magnetic field expands outward slowly due to shear while the plasma maintains its temperature due to coronal heating, then at a sufficiently large height (a few solar radii), the plasma will begin to dominate the field and expand outward indefinitely as predicted by the Parker solar wind model. Most CMEs may be just this type of pressure driven expansion. But obviously this process cannot explain the fast CMEs, which appear in the coronagraph field of view with velocities much faster than the wind, and may even slow down as they travel upward from the low corona (Sheeley *et al.* 1997). We propose that fast CMEs must be due to magnetic breakout, most likely occurring in strong active region fields.

From the viewpoint of prediction the most important feature of our model is the reconnection that must occur above the erupting arcade. This reconnection is not expected to release much energy, since most of the free magnetic energy is stored in the low-lying sheared field. Note also that the reconnection occurs on long field lines far from any neutral line. Therefore, it is unlikely to produce significant heating or strong X-ray emission, but it may be detectable in radio/microwave emission from nonthermal particles accelerated by this reconnection. We believe that radio and microwave observations will provide the best test of the magnetic breakout model for CME initiation.

This work has been supported in part by NASA and ONR.

REFERENCES

Aly, J.J. 1984, Ap.J., **283**, 349.

Aly, J.J. 1991, Ap.J., **375**, L61.

Antiochos, S.K. 1998, Ap.J., in press.

Antiochos, S.K., Dahlburg, R.B., & Klimchuk, J.A. 1994, Ap.J., **420**, L41.

Biskamp, D., & Welter, H. 1989, Solar Phys., **120**, 49.

Brueckner, G.E. 1996, EOS, Trans. AGU, **77**, S204.

DeVore, C.R. 1991, J. Comput. Phys., **92**, 142.

Finn, J.M., & Chen, J. 1990, Ap.J., **349**, 345.

Gosling, J.T. 1993, JGR, **98**, 18937.

Gosling, J.T. 1994, JGR, **99**, 4259.

Howard, R.A., Sheeley, N.R., Jr., Koomen, M.J., & Michels, D.J. 1985, JGR, **90**, 8173.

Howard, R.A., *et al.*, 1997, in **Coronal Mass Ejections: Geophysical Monograph 99**, ed. N. Crooker, J.A. Joselyn, J. Feynman, (American Geophysical Union), 17.

Hundhausen, A. J. 1997, in **Coronal Mass Ejections: Geophysical Monograph 99**, ed. N. Crooker, J.A. Joselyn, J. Feynman, (American Geophysical Union), 1.

Inhester, B., Birn, J., & Hesse, M. 1992, Solar Phys., **138**, 257.

Karpen, J.T., Antiochos, S.K., & DeVore, C.R. 1996, Ap.J., **460**, L73.

Karpen, J.T., Antiochos, S.K., & DeVore, C.R. 1998, Ap.J., **495**, 491.

Klimchuk, J.A. 1990, Ap.J., **354**, 745.

Klimchuk, J.A., & Sturrock, P. A. 1989, Ap.J., **345**, 1034.

Martin, S.F. & McAllister, A.H. 1997, in **Coronal Mass Ejections: Geophysical Monograph 99**, ed. N. Crooker, J.A. Joselyn, J. Feynman, (American Geophysical Union), 127.

McAllister, A.H., Hundhausen, A.J., & Burkepile, J.T. 1995, Bull. Am. Astron. Soc., **27**, 961.

Mikić, Z., & Linker, J. A. 1994, Ap.J., **430**, 898.

Moore, R.L. & Roumeliotis, G. 1992, *Eruptive Solar Flares*, (ed. Z. Svestka, B.V. Jackson, & M.E. Machado), (Berlin: Springer)

Low, B.C. 1994, Phys. Plasmas., **1**, 1684.

Roumeliotis, G., Sturrock, P., & Antiochos, S. 1994, Ap.J., **423**, 847.

Schwenn, R. *et al.* 1996, EOS, Trans. AGU, **77**, F558.

Steinolfson, R. S. 1991, Ap.J., **382**, 677.

Sturrock, P.A. 1989, Solar Phys., **121**, 387

Sturrock, P.A. 1991, Ap.J., **380**, 655.

Sturrock, P.A., Roumeliotis, G., & Antiochos, S.K. 1995, Ap.J., **443**, 804.

Schmieder, B., Demoulin, P., Aulanier, G., & Golub, L. 1996, Ap.J., **467**, 881.

Sheeley, N.R., Jr., *et al.* 1997, Bull. American Astron. Soc., SPD Meeting 29, No. 03.01.

Webb, D.F., Kahler, S.W., McIntosh, P.S., & Klimchuk, J.A. 1997, JGR, **102**, 24,161.

Wolfson, R. & Verma, R. 1991, Ap.J., **375**, 254.

Wolfson, R. & Low, B.C. 1992, Ap.J., **391**, 353.

Wolfson, R. & Dlamini, B. 1997, Ap.J., **483**, 961.

Wu, S.T., Guo, W.P., & Wang, J.F. 1995, Solar Phys., **157**, 325.

Yang, W.H., Sturrock, P.A., & Antiochos, S.K. 1986, Ap.J., **309**, 383.

This manuscript was prepared with the AAS LaTeX macros v4.0.